Austin Chemical Engineering

Open Access

Austin Publishing Group

Research Article

Ultrasonically Engineered Ceria-Titania Nanostructure Mediated Photocatalytic and Sonocatalytic Degradation of Organic Dye

Shah NH[1], Bhangaonkar KR[1], Pinjari DV[2] and Mhaske ST[1]*

[1]Department of Polymer and Surface Engineering, Institute of Chemical Technology, Matunga, Mumbai, India

[2]Chemical Engineering Department, Institute of Chemical Technology, Matunga, Mumbai, India

***Corresponding author:** Mhaske ST, Department of Polymer and Surface Engineering, Institute of Chemical Technology, Matunga, Mumbai, India

Received: May 04, 2016; **Accepted:** May 27, 2016; **Published:** May 30, 2016

Abstract

CeO_2, TiO_2 and CeO_2/TiO_2 composite nanoparticles were synthesized in-situ with the use of ultrasound assisted technique. The structural evaluation, its morphology and the corresponding particle size and % weight loss of the synthesized composite nanoparticles were analysed by using X-ray powder diffraction (XRD), Scanning Electron Microscopy (SEM), Transmission Electron Microscopy (TEM) and Thermo Gravimetric Analysis (TGA). Results reveal that XRD patterns have no obvious shift comparing with their standard patterns. Therefore, the oxides of TiO2 and CeO_2 should form a composite. Structure characterization of core shell particles by Transmission electron microscopy indicates that the TiO_2 shell is around 2nm in thickness and CeO_2 core is 8 nm in diameter. The effectiveness of the synthesized catalysts for the Photocatalytic as well as sonocatalytic degradation of Rhodamine B (RhB) dye has also been investigated. It has been observed that the catalytic activity of CeO_2 has been effectively increased by coating with a more photoactive TiO_2, and that photocatalysis was more efficient than sonocatalysis for the degradation of Rhodamine B.

Keywords: Sonochemical; Anosturctures; CeO_2/TiO_2; Transmission electron microscopy (TEM); Photocatalytic degradation; Sonocatalytic degradation

Introduction

Dye components are found in large quantities in the effluent waste from textile, paper, leather, cosmetics industries. The mixing of these dyes with water bodies upon disposal, leads to environmental and health related hazards [1]. Most of the organic dyes are carcinogenic and toxic in nature and hence, Photocatalytic materials that efficiently degrade the dye have been developed by various researches worldwide [2-4]. Combination of two or more materials provides the composite particle with several outstanding physical and chemical performances, especially for metal oxides [3,4]. Cerium oxide, as one of the most activity oxide catalysts in the rare earth oxide series, has the high oxygen storage capacity, redox properties, and metal support interactions [5]. CeO_2 is however, generally not considered as photoactive material [6]. Esch et al (2005) research findings about the electron localization of CeO_2 with precise observation of high-resolution scanning tunneling microscopy reveals that the defects of CeO_2 are difficult to move [7]. The results indicate inactive photo properties of CeO_2. In work reported earlier by Lin et al (2008) in order to improve activity of CeO_2 nanoparticles, CeO_2 nanoparticles have been doped with 3d transition metal ions in bulk, but it has not improved remarkably the activity of CeO_2 nanoparticles [8]. Titania is a metal oxide that is of interest for coating applications as it is widely known as useful catalyst [9,10]. Previous reports have mostly concentrated on titania coating of silica or alumina particles with diameters ranging from a few hundred nanometers to several micrometers [11,12]. Recently, coating of titania on ceria particles via conventional synthesis route has also been reported [13]. The sonochemical synthesis method is useful in synthesising nanoparticles in short time duration with higher yields. Ultrasound assisted synthesis has proven useful in deposition of nano-scaled metals and metal oxides on ceramic and polymeric particles [14-17]. Extreme reaction conditions of high temperatures of up to 5000°K and pressures up to 500 bar for a short duration in liquids with cooling rates of about 109°K/s can be obtained through the use of ultrasound, which could not possible with the use of other methods [18]. The formation, growth and implosive collapse of bubbles in a liquid medium, results in an instantaneously high temperature and pressure pulse on application of ultrasound in the liquid [19,20]. Unusual and unpredicted morphological changes are induced in the metal oxide particles due to the sound shockwaves and local intense micro mixing. Sonication also facilitates formation of more uniform shells of metal oxides of top of metallic, ceramic or polymeric cores, and is believed to significantly enhance the rate of hydrolysis [21–28]. TiO_2 being an important catalyst, we intend to synthesize CeO_2/TiO_2 composite nanoparticles, where the catalytic activity of CeO_2 can be increased by taking cooperative effects from TiO_2. Semiconductor mediated photocatalysis has been investigated extensively as a viable.

Technique for the removal of organic and inorganic pollutants from aqueous streams. The technique has proven effective for the oxidative destruction of recalcitrant organic compounds such as dyes [29]. However, photocatalysis has still not gained acceptance as an adequately efficient and effective stand-alone technology for the commercial level decontamination of wastewater [30]. Recently, Ultrasonic (US) irradiation mediated by suitable catalysts

Citation: Shah NH, Bhangaonkar KR, Pinjari DV and Mhaske ST. Ultrasonically Engineered Ceria-Titania Nanostructure Mediated Photocatalytic and Sonocatalytic Degradation of Organic Dye. Austin Chem Eng. 2016; 3(3): 1032.

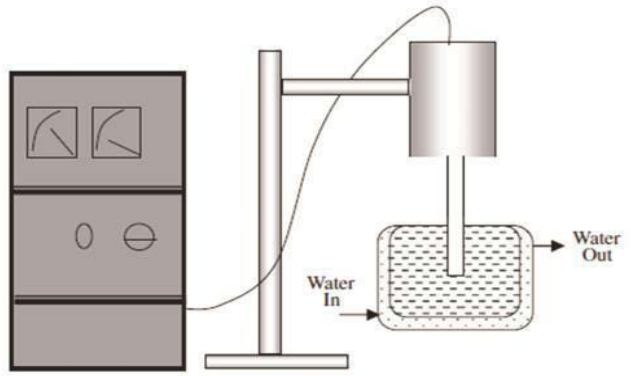

Figure 1: Ultrasound equipment set up.

(sonocatalysis) has been receiving attention as a promising technique for the treatment of hazardous organic pollutants in wastewater [31-33]. There are few reports on the preparation of individual and core/shell-type CeO_2/TiO_2 nanoparticles by ultrasound-assisted (US) technique. The present study aims to prepare individual CeO_2 and TiO_2 as well as CeO_2/TiO_2 composite nanoparticles. Additionally, it also aims at studying their Photocatalytic and sonocatalytic activity in the degradation of (Rhodamine B) RhB, to evaluate the more effective degradation technique.

Materials and Methods

Materials

Titanium Isopropoxide (TTIP) and Cerium Nitrate hexahydrate precursors and propanol solvent were obtained from S. D. Fine Chemicals Ltd., Mumbai, India. Sodium hydroxide was obtained from Merck Ltd., Mumbai, India. Rhodamine B (RhB) dye was procured from Shah Enterprises, Mumbai, India. Deionized water was used for all dilution and sample preparation. All chemical reagents are analytical grade and directly used as purchased, without further purification.

Ultrasound setup

For sonochemical synthesis technique, the ultrasound was generated with the help of a horn type ultrasonic instrument set up. The schematic of the set up is given in Figure 1. The specification and details of the set up, processing parameters used during the experiments are:

Make: Ace, USA.

Operating frequency: 22 kHz,

Rated output power: 750 W,

Diameter of stainless steel tip of horn: $1.3 * 10^{-2}$ m,

Surface area of ultrasound irradiating face: $1.32 * 10^{-4}$ m^2,

Expected ultrasound intensity $3.4*10^5$ W/m^2

Synthesis of CeO_2 via ultrasound assisted Precipitation technique

Cerium nitrate hexahydrate, 0.9g (0.1g mol) was dissolved in 30ml distilled water and 0.24g, (0.3g mol) sodium hydroxide was dissolved in 30 ml distilled water separately and was kept ready. The sodium hydroxide solution was then added drop wise to the cerium nitrate hexahydrate solution under sonication using an Ultrasonic Horn (ACE 22 kHz) at 40% amplitude for 2min with a 5s pulse and 5s relaxation cycle at time t = 0h. Precaution was taken to see to it that the addition was done in conjunction with the sonic pulse created by the transducer (Horn). After addition, the solution was again exposed to acoustic cavitation (by using ultrasonic horn) for further 18min, by keeping all sonication parameters constant (same as that was used during mixing), to carry out the complete reaction of cerium nitrate hexahydrate with sodium hydroxide. The temperature of the reaction mixture was maintained at 35 ± 2˚C by circulating water in jacketed reactor which was used for synthesis work. Further, the solution was centrifuged at 8000rpm for 10min to separate the product and the settled product was washed thrice using distilled water to remove the byproducts. After complete washing, the product was dried at 100˚C for 3h to complete the conversion of $Ce(OH)_3$ to CeO_2. After complete conversion, CeO_2 powder obtained was (light yellowish in nature), cooled, ground by mortar, and weighted to check for yield of the process.

Synthesis of TiO_2 via ultrasound assisted Sol-Gel technique

5 mL of Titanium Tetraisopropoxide (TTIP) precursor was added drop wise to 30mL of 2- propanol. The resulting clear solution was added drop wise to 5mL of glacial acetic acid solution. The mixture of TTIP precursor, 2-propanol and glacial acetic acid solution was subjected to sonication using an Ultrasonic Horn (ACE 22 kHz) at 40% amplitude actually delivering 29.2W of power for 10 min with a 5s pulse and 5 s relaxation cycle. Thus, the sol obtained after keeping it for 24h was again ultrasonically irradiated by keeping same parameters. It was then converted into a gel by adding it to 30mL of distilled water. The obtained gel was then dehydrated in an air circulating oven at 110˚C for 3h. The white powder obtained was cooled, ground and weighed to check for yield of the process.

Synthesis of CeO_2/TiO_2 composite nanoparticle via ultrasound assisted technique

The synthesis of CeO_2/TiO_2 composite nanoparticles via ultrasound assisted method, Proceeded as follows. In a typical procedure, 1.5g (0.1g mol) of $Ce(NO_3)_3.6H_2O$ was dissolved in 50ml of deionized water and 0.6g, (0.3g mol) sodium hydroxide was also dissolved in 50 ml of deionized water and kept ready. The sodium hydroxide solution was Then added drop wise to the cerium nitrate hexahydrate solution under sonication using an Ultrasonic Horn (ACE 22 kHz) at 40% amplitude for 2min with a 5s pulse and 5 s relaxation cycle at time t = 0h. Care was taken to see to it that the addition was done in conjunction with the sonic pulse afforded by the transducer (Horn). After addition, the solution was again exposed to acoustic cavitation (by using ultrasonic horn) for further 18 min, by keeping all sonication parameters constant (same as that was used during mixing), to carry out the complete reaction of cerium nitrate hexahydrate with sodium hydroxide. The temperature of the reaction mixture was maintained at 35 ± 2˚C by circulating water in jacketed reactor which was used for synthesis work. A purple colored colloidal dispersion was thus formed. 5mL of Titanium Tetraisopropoxide (TTIP) precursor was added dropwise to 30mL of 2- propanol. The resulting clear solution was added dropwise to 5mL of glacial acetic acid solution. The mixture of TTIP precursor, 2-propanol and glacial

acetic acid solution was subjected to sonication using an Ultrasonic Horn (ACE 22 kHz) at 40% amplitude actually delivering 29.2W of power for 10 min with a 5 s pulse and 5 s relaxation cycle to form a sol which was allowed to rest for 24 hours. Further, this sol was then agitated using a magnetic stirrer added drop wise to the colloidal dispersion prepared before. This mixture was further sonicated for 10min with a 5 s pulse and 5 s relaxation cycles. The resulting mixture was further centrifuged at 8000 rpm for 10min to separate the product. The separated product was dried at 110˚C for 3h. After complete conversion obtained powder was cooled, ground by mortar, and weighted to check for yield of the process.

Characterization

The phase structures of CeO_2, TiO_2, and CeO_2/TiO_2 composite nanoparticles were studied on a Rigaku Mini-Flex X-Ray Diffractometer instrument using CuKα radiation source (λ=0.154 nm). XRD patterns were recorded at angles between 20° and 80°, with a scan rate of 2°/min. Particle sizes were determined using the Debye–Scherrer equation. The thermal behavior of the composite CeO_2/TiO_2 composite nanoparticles was investigated by using thermo gravimetric analysis. The method used a Q50 TGA with standard furnace. The TGA investigation was carried out at a temperature ramp of 20°C/min, from ambient temperature (25°C) till 1000°C. Sample preparation for Scanning Electron Microscopy (SEM) includes the deposition of platinum on powder of the composite particle. The morphology and diameter of individual CeO_2 and TiO_2 composite nanoparticles were characterized by a JEOL, JSM-6380 LA 15KV Scanning electron microscope. Scanning Electron Microscopy (SEM) was carried out to provide evidence to the morphology of the individual CeO_2 and TiO_2 as well as the CeO_2/TiO_2 composite nanoparticles synthesized via US techniques. The morphology, size and structure of the particles have been investigated in detail using SEM. The morphology of CeO_2/TiO_2 composite nanoparticles and diameter of core and thickness of shell were characterized by Philips Model CM200 Transmission Electron Microscope having 177 operating voltage from 20kv to 200kv with the resolution of 2.4 A^0. The Photocatalytic and sonocatalytic degradation of RhB, using the synthesized particles as catalysts, was investigated using a Perkin–Elmer UV–visible Spectrophotometer. Demineralized water was used as a blank reference.

Photocatalytic activity

Degradation experiment: The photocatalytic activity of the individual CeO_2 and TiO_2 as well as CeO_2/TiO_2 nanoparticles as catalyst material was determined by degradation of aqueous solutions of Rhodamine B (RhB) dye, by using a photoreactor. The photoreactor is a closed box with a UV lamp Spectroline XX-15 N that emits radiation at 365 nm with intensity of 200 W/cm^2. The solution of RhB was made at 25ppm concentration each, in order to compare the activity of the composite CeO_2/TiO_2 composite nanoparticle catalyst with the photocatalytic activity of individual CeO_2 and TiO_2 nanoparticle catalysts. Solutions with 25 mg of CeO_2, TiO_2 and CeO_2/TiO_2 photocatalysts suspended in 100 ml dye solution were prepared to make aqueous solution. The experiments performed with different addition amounts showed that the photocatalytic degradation ratios of Rhodamine B gradually increase with the increase of nano-sized catalyst powder up to 25 and then the degradation of Rhodamine B reached a constant value for any additional amount of catalyst. A constant concentration of photocatalyst 0.05% was hence maintained during the degradation experiment. The suspension was subjected to irradiation under UV–vis light for a span of 90 minutes. Prior to photoreaction, the suspension was magnetically stirred in dark condition for 30 min to establish absorption/desorption equilibrium condition. Also during the photocatalytic reaction, the aqueous suspension was magnetically stirred. The solutions were exposed to ambient temperature of 35˚C and pH of 7 was maintained during the process. Aliquots of mixture were taken out with the help of a syringe at periodic intervals during the irradiation, using a micropipette. These samples were subjected to an ultracentrifuge in order to separate any suspended solids and then analysed in the double beam UV–vis spectrophotometer. The wavelength of maximum absorbance (λmax) of dye was found to be 554 nm for RhB dye. Reproducibility of the obtained experimental data is very important in investigation related to the effects of the operating parameters. In the current work, all the experiments were carried out three times to estimate the reproducibility of the obtained data. The graphs were plotted using mean values obtained from the data.

Sonocatalytic activity

Degradation experiment: The sonocatalytic activity of the individual CeO_2 and TiO_2as well as CeO_2/TiO_2 composite nanoparticles as catalyst material was determined by degradation of aqueous solutions of Rhodamine B (RhB) dye, by using an ultrasound bath. Sonocatalytic degradation process of Rhodamine B was carried out in a glass reactor filled with 100 ml of aqueous dye solution at a concentration of 25 mg/L. The experiments performed with different addition amounts showed that the sonocataytic degradation ratios of Rhodamine B tempestuously increase with the increase of nano-sized catalyst powder up to 0.05% and then the degradation ratio of Rhodamine B reached a constant value for any additional amount of catalyst. A constant concentration of sonocatalyst 0.05% was hence maintained during the degradation experiment. The suspension was magnetically stirred in dark condition for 30 min to establish absorption/desorption equilibrium condition. The solutions were exposed to ambient temperature of 35˚C and pH of 7 was maintained during the process. Ultrasonic irradiation was achieved by means of an ultrasonic bath (Dakshin Ultrasonic Model 9L 300 H/DF), which was operated at a frequency of 20 kHz and an effective power output of 80 W through manual adjusting. Under these mild ultrasonic conditions, degradation of organic substances due to ultrasound is generally reported to be quite low [35,36].

Results and Discussion

X ray diffraction (XRD)

The phase identification and structural changes were investigated with the help of X ray diffraction (XRD) technique. Figure 2 shows the typical XRD patterns recorded over 20°-80° for the all synthesized sample which gives a good insight into the crystallinity of the products. Figure 2 shows the XRD patterns for the individual as well as CeO_2/TiO_2 nanoparticles. From the XRD pattern of CeO_2/TiO_2 in Figure 2, it is seen that there are two sets of diffraction peaks for the sample, which indicates that the as-synthesized samples are composite materials. The XRD peaks at 2θ 28.541° (111) , 33.071°(200) , 47.471°(220) , 56.331°(311) , 59.071°(222) and 69.401°(400) are attributable to CeO_2 as shown in Figure 1. According to the Debye-

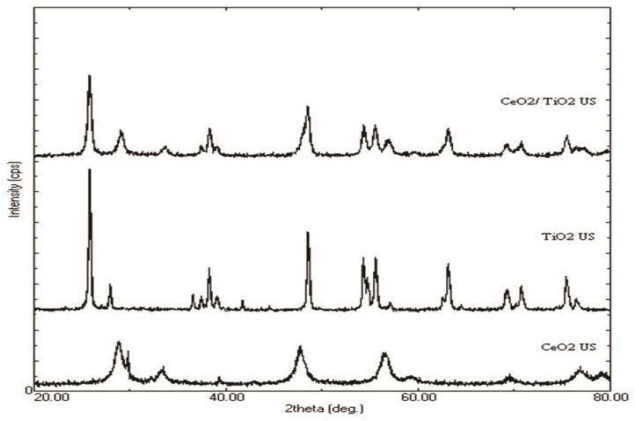

Figure 2: XRD plot of US synthesized CeO_2, TiO_2, CeO_2/TiO_2 composite nanoparticles.

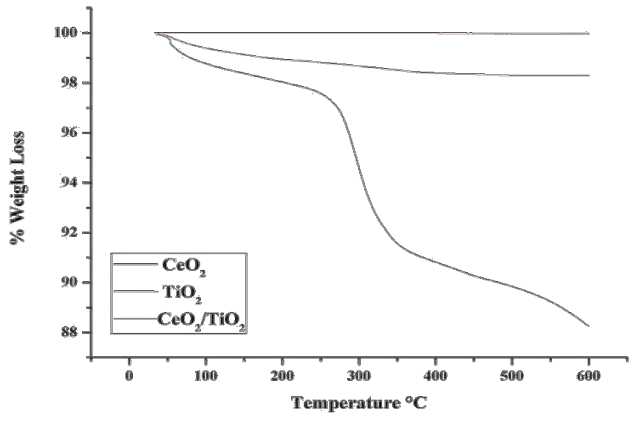

Figure 3: TGA curves of US synthesizedCeO_2, TiO_2 and CeO_2/TiO_2 nanoparticles.

Table 1: Average Crystal size and % crystallinity of US synthesized CeO_2, TiO_2, CeO_2/TiO_2 nanoparticles.

Sr No	Sample Name	% Crystallinity	Crystal size
1	US CeO_2	13.69	55.09
2	US TiO_2	40.35	57.37
3	US CeO_2 / TiO_2	28.12	30.61

Scherrer formula, the strongest peak (111) at 2θ = 28.575°, the peak (200) at 2θ = 33.139°, the peak (220) at 2θ = 47.572° and the peak (311) at 2θ = 56.402° were used to calculate the average crystal size of the CeO_2 nanoparticles, which was determined to be around 12 nm. These diffraction peaks are identified as that of pure CeO_2 consistent with JCPDS Card No.: 34-0394. The XRD peaks at 2θ 25.2° (101), 38.5° (004), 44.1° (211), 53.8° (204), 55.0° (310) are attributed to anatase TiO_2 as seen in Figure 2. These diffraction peaks are identified to be of pure anatase form of TiO_2 as per JCPDS Card No. 21-1272. The peaks at 2θ 27.4° (110), 36.0° (101), 41.2° (111), 54.3° (211) are attributed to rutile TiO_2 as seen in Figure 2. These diffraction peaks are identified to be of pure anatase form of TiO_2 as per JCPDS Card No. 21-1276. These observations indicate the presence of multiphase (anatase and rutile) form of TiO2.According to the Debye-Scherrer formula, the strongest peak (101) at 2θ = 25.2°, the peak (004) at 2θ = 38.5°, the peak (211) at 2θ = 44.1°, the peak (211) at 2θ = 54.3°, the peak (310) at 2θ = 55.0° were used to calculate the average crystal size of the TiO_2 nanoparticles, which was determined to be around 36 nm. Peak positions for both CeO_2 and TiO_2 in the XRD patterns have no obvious shift comparing with their standard patterns. Therefore, the oxides of TiO_2 and CeO_2 should form a composite. No peaks of any other phase were observed, which indicated that the product is pure and well crystallized. The following table (Table 1) summarizes the crystal sizes and % crystallinity observed in individual as well as composite core/shell particles by X - Ray diffraction.

Thermogravimetric analysis

The thermal behaviour of the CeO_2/TiO_2 composite nanoparticles synthesized by ultrasound- assisted (US) technique was investigated by using thermo gravimetric analysis. Figure 3 shows the thermo gravimetric (TGA) analysis, analyzing the weight loss of the sample with respect to a temperature gradient. A continuous weight loss was observed for the sample as the temperature was increased from 35°C to 600°C. At 50°C, it was observed that the weight loss for CeO_2/TiO_2 composite nanoparticle synthesized by US technique was 0.14% and for that of CeO_2 and TiO2 particles was 0.19% and 0%, respectively. As the samples were heated further, a notable weight loss was observed at 145°C for CeO_2/TiO_2 composite nanoparticles, which was 0.85% and for CeO_2 and TiO_2 nanoparticles it was 1.79% and 0% respectively. This loss of weight can be attributed to the disassociation of free and physically adsorbed water molecules on the nanoparticles. On heating the samples further, another notable weight loss was found at 330°C for CeO_2/TiO_2 composite nanoparticles, which was 1.42% % and for CeO_2 and TiO_2 nanoparticles it was 7.68% and 0% respectively. The reason for this reduction in weight may be the loss of chemisorbed water molecules and to dehydroxylationie loss of OH- ions from the structure. At 600°C, the final weight loss of US synthesized CeO_2/TiO_2, CeO_2 and TiO_2 nanoparticels was observed to be 1.71%, 11.75% and 0.03% respectively. Throughout the temperature gradient, the degradation characteristics of the CeO_2/TiO_2 composite nanoparticles lie between the individual CeO_2 and TiO_2 nanoparticles which suggest the formation of a composite between the two individual compounds. Ultrasound assisted technique causes a change in the crystallography of the nanoparticles. This change is caused by the formation of hotspots during acoustic cavitation and micro mixing leads to an increase in the Brownian motion of molecules. This does not allow the formation of a regular crystal structure during the core/shell particle synthesis, which leads to a reduced thermal stability of the particles synthesized using ultrasound assisted (US) technique, which may be the reason for the reduction in weight. Another reason for the weight loss exhibited by the particles synthesized using the US technique may be that sonication causes a reduction in the average particle size, which increases the efficiency of thermal conduction. Hence, at a lower temperature US particles will feel a higher effect of thermal conductive currents, which may cause a phase transformation, thus leading to the significant weight loss. This phenomenon may be investigated further, to conclusively say so.

Scanning Electron Microscopy (SEM): Figure 4 shows the SEM micrographs of the individual CeO_2, TiO_2 and CeO_2/TiO_2 nanoparticles respectively. The micrographs of the synthesized particle support the observations from the XRD patterns. SEM results

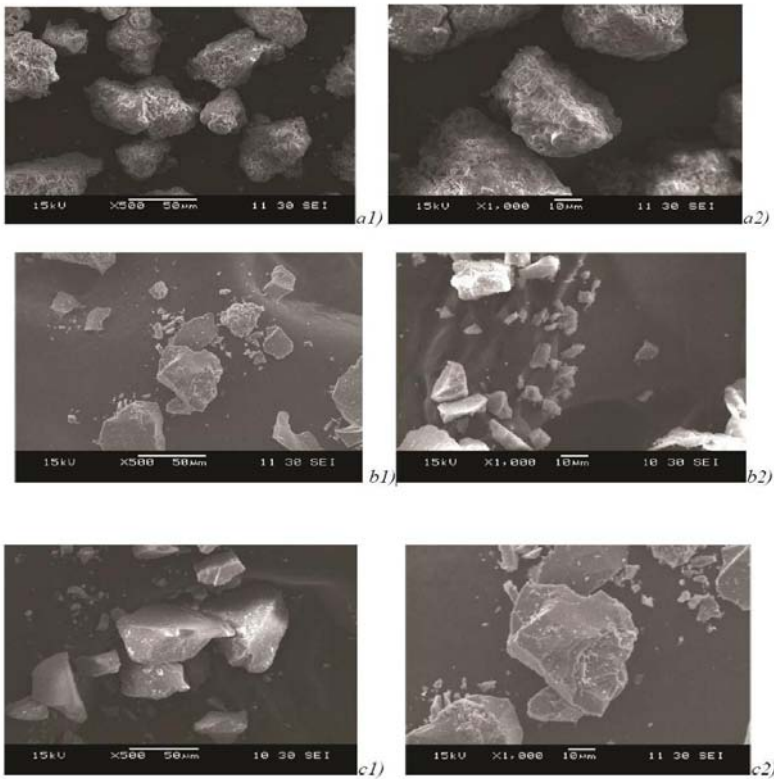

Figure 4: SEM micrographs at 500X and 1000X magnifications respectively of a 1) CeO_2 500X a 2) CeO_2 1000X, b 1) TiO_2 500X b 2) TiO_2 1000X, c 1) CeO_2/TiO_2 500X c 2) CeO_2/TiO_2 1000X nanoparticles.

were compared at the same magnification of 500X and 1000X. CeO_2 micrograph depicts the presence of agglomerated particles stacked on each other to give a rough surface morphology which you can see it from Figure 4 (a-1, & a-2). TiO_2 micrographs however indicate a smooth surface morphology from Figure 4 (b-1 & b-2). The smooth flat plate like surface of the CeO_2/TiO_2 nanoparticles as seen in the SEM image Figure 4 (c-1 & c-2) indicate that CeO_2 must have been coated with TiO_2 to impart its surface morphology. The SEM images also depict that the composite particles have smooth and sharp cuts which conforms the formation of CeO_2/TiO_2 in support to the XRD and TEM images.

Transmission electron microscopy (TEM)

Figure 5 shows the TEM image of the composite CeO_2/TiO_2 particle generated via US synthesis. The images clearly confirm the formation of CeO_2/TiO_2 composite particles, as proposed. The average size of particles as seen in the TEM graphs is in good agreement with the calculated crystallite size from XRD analysis. The dark grey or black colored portions represent the CeO_2 core, while the light grey color surrounding represents the TiO_2 shell. The particles were formed with a fairly narrow size distribution and uniform shape could be observed. The average particle size was 10 nm with the average diameter of the CeO_2 core being 8 nm and the average width of the TiO_2 coating being 2 nm. It can be clearly seen from the TEM image that the individual particles have aggregated to form secondary particles of larger size, as seen even in the SEM image (Figure 4). The aggregation can be associated to the high surface energy of the nano particles due to presence of surface charge. The

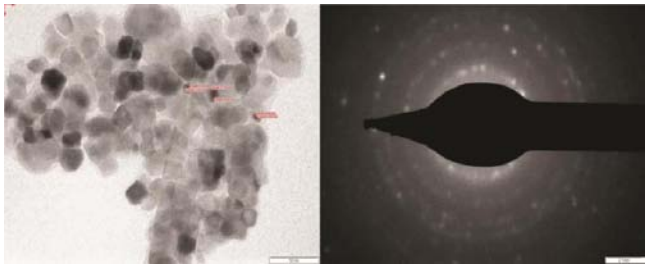

Figure 5: TEM image and SAED pattern of CeO_2/TiO_2 nanoparticles.

select area electron diffraction (SAED) patterns correspond to the CeO_2/TiO_2 nanoparticles (Figure 5). The amorphous nature of TiO_2 could be observed based on the particles and their corresponding SAED patterns.

Photocatalytic activity

The photocatalytic activity of the prepared samples was tested for the degradation of RhB constant optimum loading of photocatalyst. The effect of change in photocatalyst on the extent of degradation was investigated and has been discussed in the following sections.

Effect of change in photocatalyst: Photocatalytic activity of CeO_2, TiO_2 and CeO_2/TiO_2 core/shell photocatalysts were evaluated through the degradation of a basic dye i.e. Rhodamine B in an aqueous solution under UV radiation, as mentioned in the degradation experiment. The removal of Rhodamine B in the presence of all three type of catalyst powders was confirmed by a drop in the absorbance peak within visible wavelength as shown in Figure 6.

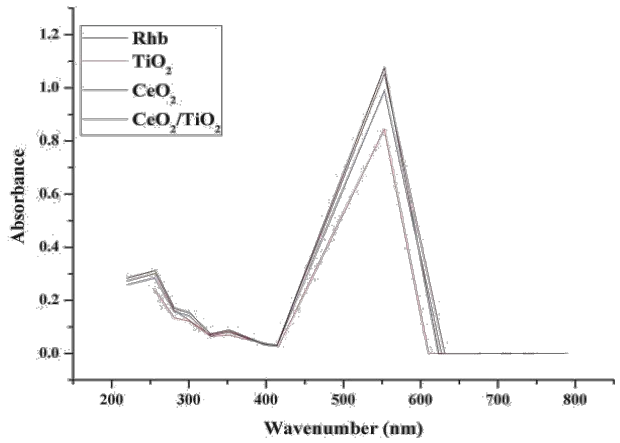

Figure 6: UV-vis spectra of RhB during photocatalytic degradation.

Abs vsλ for RhB proving λmax = 554 nm

It has been reported by Minero et al. [34], that when the alteration of the shape of the spectrum is not significant, it indicates that there is no colored degradation intermediates produced. Thus, the spectral interference during our reaction was negligible and the change in absorbance value can be due to dye degradation in presence of photocatalyst, after 90mins. The concentration of Rhodamine B was detected at its maximum absorbance of 554 nm as found from the absorption peak in Figure 6. The degradation efficiency of Rhodamine B is defined as follows:

Degradation efficiency (%) = $\{C_0 - C_t)/C_0 \times 100\%$

where C_0 is the initial concentration of Rhodamine B and Ct is the concentration of Rhodamine B at reaction time t (min). Figure 7 shows the comparison of degradation efficiency rhodamine B in the presence of the synthesized nano-sized powders, under UV radiation at different moments. It can be seen that the concentration of rhodamine B solutions gradually decrease along with irradiation time, which indicates that rhodamine B in aqueous solutions is decomposed piece by piece under UV light. The detailed degradation processes are shown in Figure 8. It could be seen that the degradation ratio of Rhodamine B in the presence of nano-sized CeO_2 powder

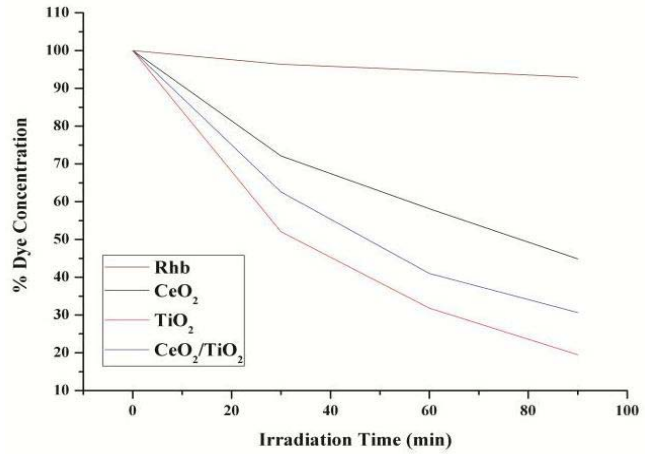

Figure 7: Degradation of RhB with respect to time in presence of photocatalyst.

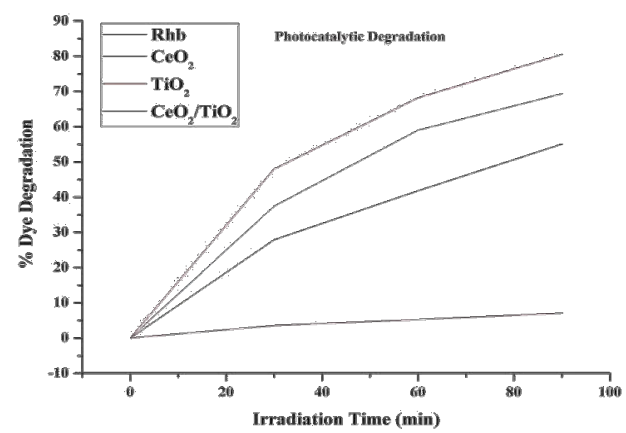

Figure 8: Effect of photocatalyst on degradation of RhB.

attains 55.11% within 90 minutes of exposure to UV light, while it was 80.51% for rhodamine B in presence of TiO_2 and 69.35% in presence of composite CeO_2/TiO_2 nano-sized photocatalyst, respectively, at the same time. Correspondingly, the degradation ratio of rhodamine B in the absence of any catalyst under only UV irradiation was only 7.05% at the same moment. These results indicate that the degradation effects of rhodamine B in the presence of nano-sized catalyst powders combining with UV light are more obvious than corresponding to those using only UV light. The increase in the degradation rate in the presence of catalyst can be attributed to the semiconducting nature of the catalyst particles. Irradiation of metal oxide particles with photons of energy equal to, or greater than their band gap energy, results in the promotion of an electron from the Valence Band (VB) to the Conduction Band (CB) of the particle. The outcome of this process is a region of positive charged hole, in the valance band. The charge can migrate to the particle surface, where the holes can react with surface-bound hydroxyl groups (OH^-) and adsorbed water molecules to form hydroxyl radicals (OH•) ie carry out water dissociation reaction. The high intensity of UV light generated in the reactor leads to generation of large amount of free radicals in the aqueous system, hence causing an increased degradation. In addition, to infer the reaction kinetics of photocatalytic degradation of rhodamine B, the data of -ln (C_t/C_0) for first-order reaction as a function of irradiation time (t) were calculated. In Figure 9, the results indicate that all calculated values of -ln (C_t/

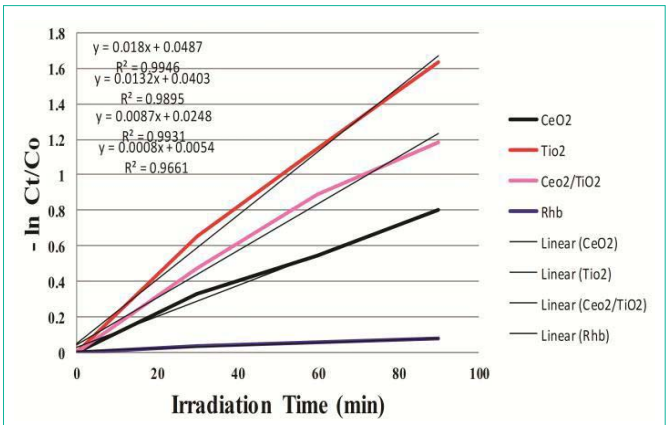

Figure 9: Influence of photocatalyst on rate of degradation of RhB.

C_0) are approximately linear with the irradiation time all through for photocatalytic degradation of Rhodamine B for all cases; ie they conform to pseudo first-order kinetics reactions. The rate constants of photo degradation processes of rhodamine B in presence of CeO_2, TiO_2 and CeO_2/TiO_2 composite particles are much larger than that of photo degradation of RhB solution without catalysts. This supports our intention for synthesis of photocatalytic materials for degradation of RhB dye. The Photocatalytic activities of these nanoparticles show significant differences. That is, the order of Photocatalytic activities is TiO_2 > CeO_2/TiO_2 > CeO_2. The corresponding degradation ratios calculated are 80.51%, 69.35% and 55.11%, respectively, and that the degradation ratio under UV radiation alone is only 7.05%. The result confirms the intention of coating CeO_2 particles with more reactive TiO_2, to increase its photocatalytic activity.

Sonocatalytic activity

Aliquots of mixture were taken out at periodic intervals during the irradiation, using a micropipette. These samples were subjected to an ultracentrifuge in order to separate any suspended solids and then analyzed in the double beam UV–v is spectrophotometer. The wavelength of maximum absorbance (λmax) of dye was found to be 554 nm for RhB dye. Reproducibility of the obtained experimental data is very important in investigation related to the effects of the operating parameters. In the current work, all the experiments were carried out three times to estimate the reproducibility of the obtained data. The graphs were plotted using mean values obtained from the data.

Effect of change in sonocatalyst: Sonocatalytic activity of CeO_2, TiO_2 and CeO_2/TiO_2 core/shell sonocatalysts was evaluated through the degradation of a basic dye i.e. Rhodamine B in an aqueous solution under ultrasonic irradiation as mentioned in the degradation experiment. The removal of Rhodamine B in the presence of all three type of catalyst powders was confirmed by a drop in the absorbance peak within visible wavelength as shown in Fig. 10. It has been reported by Minero et al. [34], that when the alteration of the shape of the spectrum is not significant, it indicates that there is no colored degradation intermediates produced. Thus, the spectral interference during our reaction was negligible and the change in absorbance value can be due to dye degradation in presence of sonocatalyst, after 90 mins. The concentration of Rhodamine B was detected at its maximum absorbance of 554 nm as found from the absorption peak in Figure 10. The degradation efficiency of Rhodamine B is defined as follows:

$$\text{Degradation efficiency (\%)} = \{C_0 - C_t)/C_0 \times 100\%$$

Where, C_0 is the initial concentration of Rhodamine B and Ct is the concentration of Rhodamine B at reaction time t (min). Figure 11 shows the comparison of degradation efficiency Rhodamine B in the presence of the synthesized nano-sized powders, under ultrasonic irradiation at different moments. It can be seen that the absorption peaks of Rhodamine B solutions gradually decrease along with irradiation time, which indicates that Rhodamine B in aqueous solutions is decomposed piece by piece under ultrasonic irradiation. The detailed degradation processes are shown in Figure 12. It could be seen that the degradation ratio of Rhodamine B in the presence of nano-sized CeO_2 powder attains 36.82% within 90 minutes of ultrasonic irradiation, while it was 58.96% for Rhodamine B in presence of TiO_2 and 46.41% in presence of composite CeO_2/TiO_2 nano-sized sonocatalyst, respectively, at the same time. Correspondingly, the degradation ratio of Rhodamine B in the absence of any catalyst under only ultrasound irradiation was only 13.9% at the same moment. These results indicate that the degradation effects of Rhodamine B in

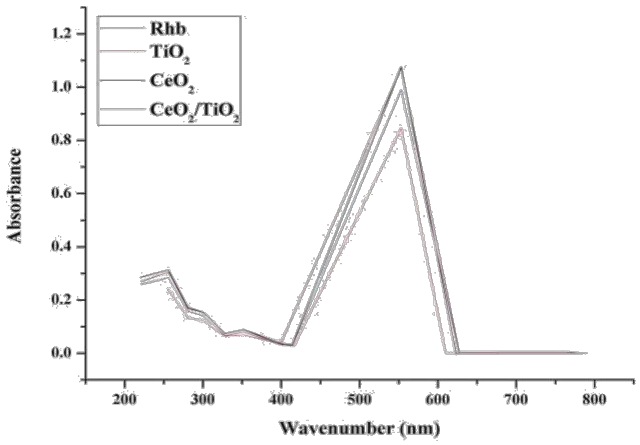

Figure 10: UV-vis spectra of RhB during sonocatalytic degradation.

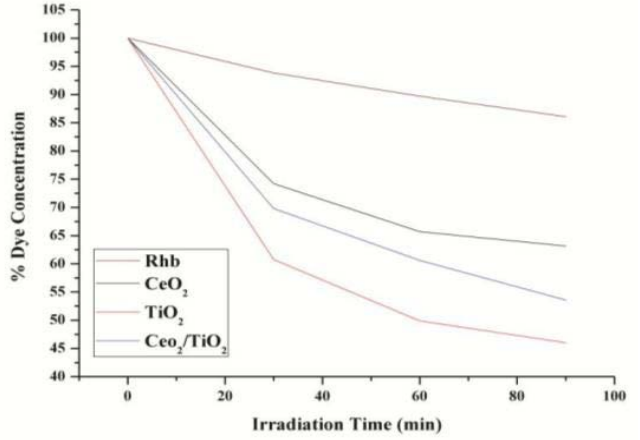

Figure 11: Degradation of RhB with respect to time in presence of sonocatalyst.

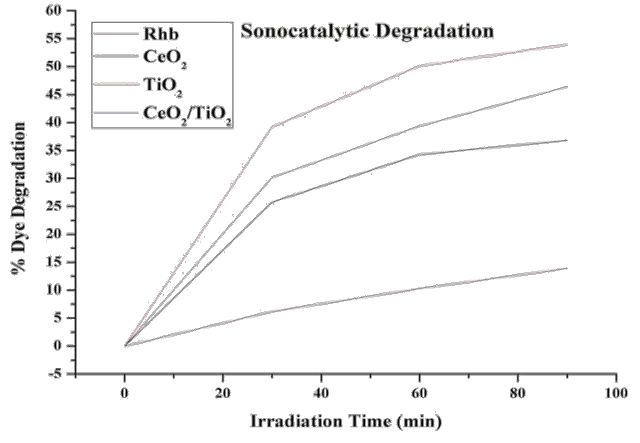

Figure 12: Effect of sonocatalyst on degradation of RhB.

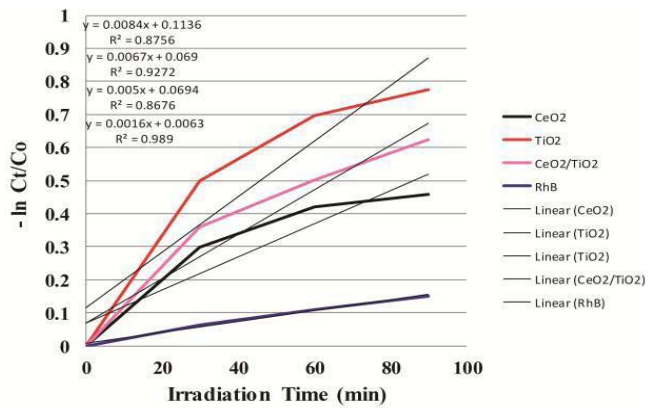

Figure 13: Influence of sonocatalyst on rate of degradation of RhB.

the presence of nanosized catalyst powders combining with ultrasonic irradiation are more obvious than corresponding to those using one fold ultrasonic irradiation. The increase in the degradation rate in the presence of catalyst can be attributed to the presence of solid particles in a liquid which increased the nucleation sites for cavity formation. Once undergoing electron shifts from the valence band to the conduction band, the metal oxide particles itself could also act as a catalyst to promote water dissociation reactions. The combined effects led to the generation of more free radicals in the aqueous system, hence causing an increased degradation. In addition, to infer the reaction kinetics of sonocatalytic degradation of rhodamine B, the data of -ln (C_t/C_0) for first-order reaction as a function of irradiation time (t) were calculated. In Figure 13, the results indicate that all calculated values of -ln (C_t/C_0) are approximately linear with the irradiation time all through for sonocatalytic degradation of Rhodamine B for all cases ie they conform to pseudo first-order kinetics reactions. Nevertheless, the rate constants of degradation processes for ultrasonic irradiation of rhodamine B in presence of CeO_2, TiO_2 and CeO_2/TiO_2 composite particles are much larger than that of RhB solution without catalysts. This supports our intention for synthesis of sonocatalytic materials for degradation of RhB dye. The sonocatalytic activities of these nanoparticles show significant differences. That is, the order of sonocatalytic activities is TiO_2 > CeO_2/TiO_2 > CeO_2. The corresponding degradation ratios calculated are 53.96%, 46.41% and 36.82% respectively. And that the degradation ratio under ultrasonic irradiation alone is only 13.9%. The results demonstrate that CeO_2/TiO_2 composite takes co-operative effects from individual components to demonstrate sonocatalytic activity at the used intensity and frequency of ultrasound.

Conclusion

Nano-sized CeO_2, TiO_2 and CeO_2/TiO_2 particles were successfully prepared via eco-friendly ultrasound-assisted technique. The evidence of formation of CeO_2/TiO_2 core/shell is given by the TEM images. The as prepared particles were further tested for its catalytic activity by using Rhodamine B dye. Degradation characteristics confirmed the inferior catalytic activity of CeO_2 nanoparticles in comparison to TiO_2 nanoparticles and thus support our intention of coating CeO_2 particles with a TiO_2 shell to increase the activity of CeO_2 as a catalyst. Superior photocatalytic degradation over sonocatalytic degradation was also confirmed by higher % degradation of Rhodamine B and rate of reaction.

References

1. L Kong, X Gan, A Ahmad, B Hamed, E R Evarts, B Ooi, et al. Design and synthesis of magnetic nanoparticles augmented microcapsule with catalytic and magnetic bifunctionalities for dye removal. Chem. Eng. J. 2012; 197: 350-358.
2. FC Wu, R L Tseng. High adsorption capacity NaOH-activated carbon for dye removal from aqueous solution. J.Hazard. Mater. 2008; 152: 1256-1267.
3. MH Liao, CH Hsu, DH Chen. Preparation and properties of amorphous titania-coated zinc oxide anoparticles, Journal of Solid State Chemistry. 2006; 179: 2020-2026.
4. Xiaogang Peng, Michael C Schlamp, Andreas V Kadavanich, and A P Alivisatos. Epitaxial Growth of Highly Luminescent CdSe/CdS Core/Shell Nanocrystals with Photostability and Electronic Accessibility. J. Am. Chem. Soc. 1997; 119: 7019-7029.
5. Xiaofei Qu, Dandan Xie, Lei Gao, Fanglin Du. Synthesis and photocatalytic activity of TiO_2/CeO_2 core–shell nanotubes. Materials Science in Semiconductor Processing. 2014; 26: 657-662.
6. Ningning Yan, Zhongqi Zhu, Jin Zhang, Zongyan Zhao, Qingju Liu. Preparation and properties of ce-doped TiO_2 photocatalyst. Materials Research Bulletin. 2012; 47: 1869-1873.
7. Esch F, Fabris S, Zhou L, Montini T, Africh C, Fornasiero P, et al. Electron localization determines defect formation on ceria substrates. Science. 2005; 309: 752-755.
8. Caimei Fan, Peng Xue, Yanping Sun. Preparation of Nano-TiO_2 Doped with Cerium and Its Photocatalytic Activity. Journal of Rare Earths. 2006; 24: 309-313.
9. D Tomova, V Iliev, A Eliyas, S Rakovsky. Promoting the oxidative removal rate of oxalic acid on gold-doped CeO_2/TiO_2 photocatalysts under UV and visible light irradiation. Separation and Purification Technology. 2015; 156: 715-723.
10. Chunjing Hao, Jing Li, Zailei Zhang, Yongjun Ji, Hanhui Zhan, Fangxing Xiao, et al. Enhancement of photocatalytic properties of TiO_2 nanoparticles doped with CeO_2 and supported on SiO_2 for phenol degradation. Applied Surface Science. 2015; 331: 17-26.
11. Yangang Wang, Bo Li, Chengli Zhang, Lifeng Cui, Shifei Kang, Xi Li, et al. Ordered mesoporous CeO_2-TiO_2 composites: Highly efficient photocatalysts for the reduction of CO_2 with H_2O under simulated solar irradiation. Applied Catalysis B: Environmental. 2013; 130: 277-284.
12. Zhong Z, Yin Y, Gates B, Xia Y. Preparation of Mesoscale Hollow Spheres of TiO_2 and SnO_2 by Templating Against Crystalline Arrays of Polystyrene Beads. Adv Mater. 2000; 12: 206-209.
13. Yue lin, Zhang Xiaoming. Preparation of highly dispersed CeO_2/TiO_2 core-shell nanoparticles. material letters. 2008; 62: 3764-3766.
14. KS Suslick, GJ Price. Applications of ultrasound to material chemistry. Annu. Rev. Mater. 1999; 29: 295.
15. A Gedanken. Using sonochemistry for the fabrication of nanomaterials. Ultrason Sonochem. 2004; 11: 47-55.
16. VG Pol, DN Srivastava, O Palchik, V Palchik, MA Slifkin, AM Weiss, et al. Sonochemical deposition of silver nanoparticles on silica spheres. Langmuir. 2002; 18: 3352-3357.
17. N Perkas, G Amirian, S Dubinsky, S Gazit, A Gedanken. Ultrasound- assisted coating of nylon6,6 with silver nanoparticles and its antibacterial activity. Appl Polym. Sci. 2007; 104: 1423-1430.
18. F Dang, N Enomoto, J Hojo, K Enpuku. Sonochemical coating of magnetite nanoparticles with silica. Ultrason. Sonochem. 2010; 17: 193-199.
19. VS Moholkar, SP Sable, AB Pandit. Mapping the cavitation intensity in an ultrasonic bath using the acoustic emission. AIChE J. 2000; 46: 684-694.
20. AV Mahulkar, C Riedel, PR Gogate, U Neis, AB Pandit. Effect of dissolved gas on efficacy of sonochemical reactors for microbial cell disruption: experimental and numerical analysis. Ultra Sonochem. 2009; 16: 635-643.

21. JH Bang, KS Suslick. Applications of ultrasound to the synthesis of nanostructured materials. Adv. Mater. 2010; 22: 1039-1059.

22. NA Dhas, KS Suslick. Sonochemical preparation of hollow nano-spheres and hollow nanocrystals. J.Am. Chem. Soc. 2005; 127: 2368-2369.

23. VG Pol, M Motiei, A Gedanken, J Calderon-Moreno, Y Mastai. Sonochemical deposition of air-stable iron nanoparticles on monodispersed carbon spherules. Chem.Mater. 2003; 15: 1378-1384.

24. N Ghows, MH Entezari. Fast and easy synthesis of core–shell nanocrystals (CdS/TiO_2) at low temperature by micro-emulsion under ultrasound. Ultrason. Sonochem. 2011; 18: 629- 634.

25. Yun Wang, Jie Zhao, Tianfu Wang, Yingxuan Li, Xiyou Li, Jiao Yin, et al. CO_2 hotoreduction with H_2O vapor on highly dispersed CeO_2/TiO_2 catalysts: Surface species and their reactivity. Journal of Catalysis. 2016; 337: 293-302.

26. JP Park, SK Kim, JY Park, S Ahn, KM Ok, HY Kwak, et al. Coating of TiO_2 nanoparticles with PbS thin films and preparation of PbS nanoparticles using a one-pot sonochemical reaction under the multi bubble sono luminescence conditions. Thin Solid Films. 2009; 517: 6663-6665.

27. N Ghows, MH Entezari. Sono-synthesis of core–shell nanocrystal (CdS/TiO_2) without surfactant. Ultrason. Sonochem. 2012; 19: 1070-1078.

28. N Perkas, G Amirian, C Rottman, F delaVega, A Gedanken. Sonochemical deposition of magnetite on silver nanocrystals. Ultrason. Sonochem. 2009; 16: 132-135.

29. MST Gonsalves, AMF Oliveira-Campose, EMMS Pinto, PMS Plasencia, MJRP Queiroz. Photochemical treatment of solutions of azo dyes containingTiO_2. Chemosphere. 1999; 39: 781-786.

30. SG Anju, SugunaYesodharan, EP Yesodharan. Zinc oxide mediated sonophotocatalytic degradation of phenol in water. Chemical Engineering Journal. 2012; 189: 84- 93.

31. ZD Meng, WC Oh. Sonocatalytic degradation and catalytic activities for MB solution of Fe treated fullerene/TiO_2 composite with different ultrasonic intensity. Ultrason. Sonochem. 2011; 18: 757-764.

32. S Marouani, O Hamdaoui, F Saoudi, M Chiha. Sonochemical degradation of Rhodamine B in aqueous phase. Effect of additives, Chem. Eng. J. 2010; 158: 550-557.

33. L Song, C Chen, S Zhang. Sonocatalytic performance of Tb_7O_{12}/TiO_2 underultrasonic irradiation. Ultrason. Sonochem. 2011; 18: 713-717.

34. C Minero, P Pellizzari, V Maurino, E Pelizzetti, D Vione. Enhancement of Dye Sonochemical Degradation by Some Inorganic Anions Present in Natural Waters. Appl. Catal. B: Environ. 2008; 77: 308-316.

35. Xiaowang Lu, Xiazhang Li, Junchao Qian, Naiming Miao, Chao Yao, Zhigang Chen. Synthesis and characterization of CeO_2/TiO_2 nanotube arrays and enhanced photocatalytic oxidative desulfurization performance. Journal of Alloys and Compounds. 2016; 661: 363-371.

36. J Wang, Z Jiang, Z Zhang, Y Xie, X Wang, Z Xing, et al. Sonocatalytic degradation of acid red B and rhodamine B catalyzed by nano-sized ZnO powder under ultrasonic irradiation. ltrason Sonochem. 2008; 15: 768-774.

Austin Chem Eng - Volume 3 Issue 3 - 2016
ISSN : 2381-8905 | www.austinpublishinggroup.com

Citation: Shah NH, Bhangaonkar KR, Pinjari DV and Mhaske ST. Ultrasonically Engineered Ceria-Titania Nanostructure Mediated Photocatalytic and Sonocatalytic Degradation of Organic Dye. Austin Chem Eng. 2016; 3(3): 1032.